the plant journal

SEB Society for Experimental Biology

The Plant Journal (2015) **81,** 53–67 doi: 10.1111/tpj.12692

Arabidopsis acyl-CoA-binding protein ACBP3 participates in plant response to hypoxia by modulating very-long-chain fatty acid metabolism

Li-Juan Xie†, Lu-Jun Yu†, Qin-Fang Chen†, Feng-Zhu Wang, Li Huang, Fan-Nv Xia, Tian-Ren Zhu, Jian-Xin Wu, Jian Yin, Bin Liao, Nan Yao, Wensheng Shu and Shi Xiao*

State Key Laboratory of Biocontrol and Guangdong Key Laboratory of Plant Resources, School of Life Sciences, Sun Yat-sen University, Guangzhou 510275, China

Received 6 August 2014; revised 21 September 2014; accepted 29 September 2014; published online 6 October 2014.
*For correspondence (e-mail xiaoshi3@mail.sysu.edu.cn).
†These authors contributed equally to this work.

SUMMARY

In *Arabidopsis thaliana*, acyl-CoA-binding proteins (ACBPs) are encoded by a family of six genes (*ACBP1* to *ACBP6*), and are essential for diverse cellular activities. Recent investigations suggest that the membrane-anchored ACBPs are involved in oxygen sensing by sequestration of group VII ethylene-responsive factors under normoxia. Here, we demonstrate the involvement of Arabidopsis ACBP3 in hypoxic tolerance. *ACBP3* transcription was remarkably induced following submergence under both dark (DS) and light (LS) conditions. *ACBP3*-overexpressors (*ACBP3-OEs*) showed hypersensitivity to DS, LS and ethanolic stresses, with reduced transcription of hypoxia-responsive genes as well as accumulation of hydrogen peroxide in the rosettes. In contrast, suppression of *ACBP3* in *ACBP3-KOs* enhanced plant tolerance to DS, LS and ethanol treatments. By analyses of double combinations of *OE-1* with *npr1-5*, *coi1-2*, *ein3-1* as well as *ctr1-1* mutants, we observed that the attenuated hypoxic tolerance in *ACBP3-OEs* was dependent on NPR1- and CTR1-mediated signaling pathways. Lipid profiling revealed that both the total amounts and very-long-chain species of phosphatidylserine (C42:2- and C42:3-PS) and glucosylinositolphosphorylceramides (C22:0-, C22:1-, C24:0-, C24:1-, and C26:1-GIPC) were significantly lower in *ACBP3-OEs* but increased in *ACBP3-KOs* upon LS exposure. By microscale thermophoresis analysis, the recombinant ACBP3 protein bound VLC acyl-CoA esters with high affinities *in vitro*. Further, a knockout mutant of MYB30, a master regulator of very-long-chain fatty acid (VLCFA) biosynthesis, exhibited enhanced sensitivities to LS and ethanolic stresses, phenotypes that were ameliorated by *ACBP3-RNAi*. Taken together, these findings suggest that Arabidopsis ACBP3 participates in plant response to hypoxia by modulating VLCFA metabolism.

Keywords: acyl-CoA-binding proteins, *Arabidopsis thaliana*, hypoxic tolerance, sphingolipids, very-long-chain fatty acids.

INTRODUCTION

Flooding is one of the most important abiotic stresses of worldwide concern that determines crop productivity, geographic distribution of plant species and abundance of natural ecosystems (Perata and Voesenek, 2007). Flooding events including root waterlogging and submergence markedly affect diffusion of gases into plant cells, which eventually leads to hypoxia, and carbohydrate shortages in terrestrial plants (Geigenberger, 2003; Bailey-Serres and Voesenek, 2008, 2010; Voesenek and Bailey-Serres, 2013). In response to flooding, plants develop aerenchyma and adventitious roots to facilitate gas exchange, or shift from aerobic to anaerobic metabolism to sustain survival (Bailey-Serres and Voesenek, 2008). With increasing anaerobic respiration, the accumulation of toxic metabolites such as lactic acid, acetaldehyde and ethanol cause damage to plant cells. Moreover, the accumulation of reactive oxygen species (ROS) during re-oxygenation upon subsiding of floodwaters can cause further injury to plant tissues (Bailey-Serres and Voesenek, 2008; Voesenek and Bailey-Serres, 2013).

In recent years, considerable progress has been made in understanding how plants sense and respond to hypoxic stress. For example, many hypoxia-responsive genes and related microRNAs have been identified in Arabidopsis

and *Zea mays* through genomic technologies (Chang *et al.*, 2000; Klok *et al.*, 2002; Licausi *et al.*, 2011b; Mithran *et al.*, 2013). Phenotypic analyses of attenuated or enhanced hypoxic tolerant mutants and transgenic lines demonstrated that four members of the group VII ethylene response transcription factors (ERFs), including ERF73/HRE1, ERF71/HRE2, RAP2.2, and RAP2.12, are positive regulators of the hypoxia response in Arabidopsis (Hinz *et al.*, 2010; Licausi *et al.*, 2010, 2011b; Yang *et al.*, 2011). Moreover, homeostatic hypoxia sensing is tightly regulated by RAP2.12, via the N-end rule proteolysis pathway (Gibbs *et al.*, 2011; Licausi *et al.*, 2011a). In this model, under normoxic conditions, the RAP2.12 protein is subcellularly associated with the plasma membrane by interacting with two membrane-anchored acyl-CoA-binding proteins ACBP1 and ACBP2 (Licausi *et al.*, 2011a; Bailey-Serres *et al.*, 2012). Upon hypoxia, RAP2.12 is released and translocates to the nucleus to activate the transcription of hypoxia-responsive genes. During re-oxygenation following hypoxia, the RAP2.12 protein is rapidly ubiquitinated and proteolytically degraded thereby terminating hypoxia signaling (Licausi *et al.*, 2011a; Bailey-Serres *et al.*, 2012). Besides, ACBP2 and cytosolic ACBP4 proteins were found to interact with another member of group VII ERFs, RAP2.3/AtEBP (Li and Chye, 2004; Li *et al.*, 2008), whose biological significance in hypoxia response is yet to be determined. It is therefore conceivable that ACBPs or ACBP-associated lipids may play crucial roles in hypoxia signaling in plants.

Lipids are essential cellular constituents that not only provide the structural basis for cell membranes and energy for metabolic processes, but also serve as signals in plant responses to environmental cues (Wang, 2004). ACBP proteins are a family of lipid-binding proteins conserved in eukaryotic and prokaryotic organisms, which show ability to bind acyl-CoA esters and phospholipids via the acyl-CoA-binding (ACB) domain (Burton *et al.*, 2005; Xiao and Chye, 2011a). In addition to the conventional 10-kDa cytosolic ACBPs, recent investigations have identified several larger proteins with the ACB domain from both mammals and plants (Xiao and Chye, 2009, 2011a; Fan *et al.*, 2010; Yurchenko and Weselake, 2011). In Arabidopsis, there are six genes encoding ACBP proteins with different subcellular localizations. Among them, the small 10-kDa ACBP6 is involved in phospholipid metabolism by interacting with phosphatidylcholine (PC), and its overexpression confers freezing tolerance in Arabidopsis (Chen *et al.*, 2008). The five larger forms of ACBP (designated ACBP1 to ACBP5) range in size from 37.5 to 73.1 kDa and show distinct binding affinities to acyl-CoA esters and phospholipids (Xiao and Chye, 2009, 2011a; Du and Chye, 2013). More recently, the functions of these ACBP proteins have been intensely explored by reverse genetics and biochemical approaches (Xiao and Chye, 2011a). In particular, the existence of ankyrin repeats in ACBP1 and ACBP2, and a kelch motif present in ACBP4 and ACBP5, enables these proteins to interact with various protein partners (Du and Chye, 2013). To date, the identified targets for ACBP1 and ACBP2 include the ethylene-responsive factors RAP2.3/AtEBP and RAP2.12 (Li and Chye, 2004; Licausi *et al.*, 2011a), heavy-metal-binding protein AtFP6 (Gao *et al.*, 2009), lysophospholipase LysoPL2 (Gao *et al.*, 2010), phospholipase PLDα1 (Du *et al.*, 2013) and ABA-responsive-element-binding protein1 AREB1 (Du and Chye, 2013). It is interesting to note that all these ACBP1 and/or ACBP2 interactors are stress-responsive proteins or transcription factors, which indicates that ACBPs are involved in stress tolerance by either binding to differential acyl-CoAs/lipids or combining with other protein interactors.

Arabidopsis ACBP3 is a unique protein that possesses an ACB domain and an overlapping N-terminal transmembrane domain with extracellular-targeting signal peptides, ensuring ACBP3 is directed to the extracellular region and within intracellular membranes (Xiao *et al.*, 2010). Overexpression of *ACBP3* accelerates age-dependent and starvation-triggered leaf senescence through binding to phosphatidylethanolamine (PE), an interaction that is confirmed to interfere with the PE lipidation of the autophagy-related protein ATG8 (Xiao *et al.*, 2010). Moreover, *ACBP3* overexpression constitutively activates the expression of pathogenesis-related (*PR*) genes, induces cell death and leads to accumulation of hydrogen peroxide (H_2O_2) and salicylic acid (SA) in the rosettes (Xiao and Chye, 2011b). Observations that *ACBP3*-overexpressors (*ACBP3-OEs*) display enhanced resistance to the hemi-biotrophic pathogens, but greater susceptibility to the necrotrophic pathogens (Xiao and Chye, 2011b), support a role for ACBP3 in SA-dependent plant defense signaling.

In this study, *ACBP3* gene expression was remarkably induced by submergence under both dark (DS) and light (LS) conditions. *ACBP3-OEs* attenuated plant resistance, whereas down-regulation of *ACBP3* (*ACBP3-KOs*) enhanced plant tolerance to DS, LS and ethanolic applications. Moreover, the phenotypes of *ACBP3-OEs* and *ACBP3-KOs* were correlated with dynamic changes of VLCFA-containing phospholipids and sphingolipids. In addition, recombinant ACBP3 (rACBP3) protein was shown to bind VLC acyl-CoA esters with high affinities *in vitro*. These findings suggest that ACBP3 is involved in plant response to hypoxic stress by modulating VLCFA metabolism.

RESULTS

The expression patterns of Arabidopsis *ACBPs* upon hypoxia exposure

To determine the involvement of Arabidopsis *ACBPs* in hypoxia response, 4-week-old plants were subjected to DS or darkness alone as a control (Dark), and the transcript

profiles of six *ACBPs* were determined by real-time quantitative reverse transcription PCR (qRT-PCR) analysis. The expression of *ACBP3* was significantly induced but the levels of *ACBP4* and *ACBP5* were significantly repressed by exposing Arabidopsis plants to the extended darkness (Figure 1a), which is consistent with previous observations (Xiao and Chye, 2009; Xiao *et al.*, 2010). Upon DS exposure, *ACBP3* transcription was significantly elevated, with levels increasing 24.3- to 94.5-fold from 3 to 24 h (Figure 1a). Expression of *ACBP6* was also slightly inducible by darkness and was further up-regulated at 6, 9 and 12 h after DS treatment. Both *ACBP2* and *ACBP5* mRNA levels were elevated at 6 h under DS. Whereas the level of *ACBP2* had further increased, the level of *ACBP5* had decreased at 12 h after treatment (Figure 1a). In contrast, the expression of *ACBP1* and *ACBP4* was not responsive to DS.

To uncouple the effects of darkness on the DS-affected expression of *ACBPs*, Arabidopsis plants were submerged under LS and the expression levels of *ACBPs* were examined. Consistently, *ACBP3* was induced at 3, 6, 9, 12 and 24 h after LS treatment, with the highest expression

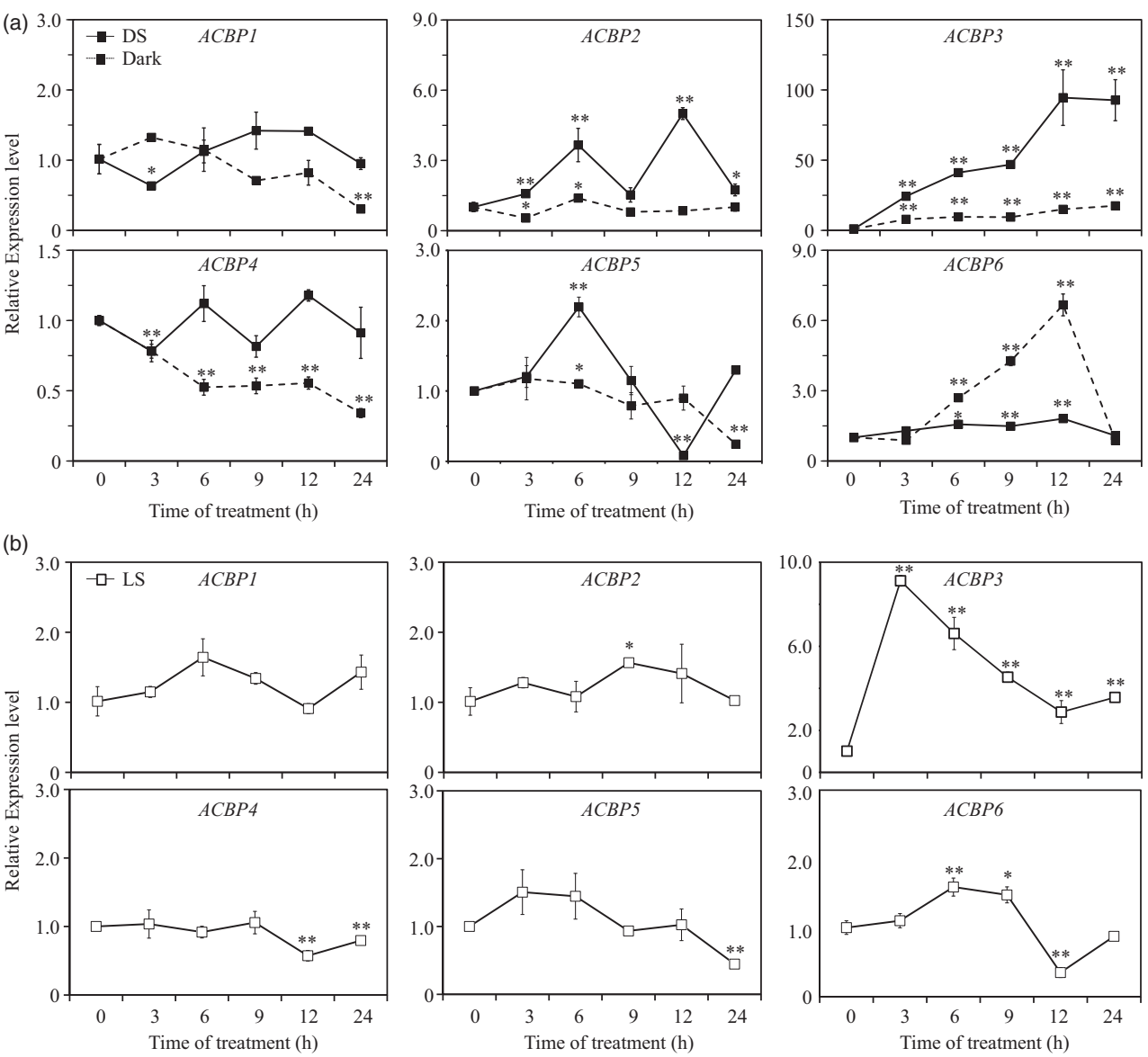

Figure 1. Expression profiles of Arabidopsis *ACBPs* under submergence.
Total RNA was extracted from 4-week-old soil-grown seedlings upon dark and DS (a), or LS (b) treatment. The samples were harvested at 0, 3, 6, 9, 12 or 24 h after treatment, and the relative expression levels of Arabidopsis *ACBPs* (*ACBP1* to *ACBP6*) were determined by qRT-PCR. Expression levels relative to 0 h for each time point were normalized to that of *ACTIN2.* Data are means ± SD of three independent replicates. Asterisks indicate significant difference from untreated control (0 h); $*P < 0.05$; $**P < 0.01$ by Student's *t*-test. The experiment was repeated with similar results.

occurring at 3 h (Figure 1b). However, transcription of *ACBP1*, *ACBP2*, *ACBP4*, *ACBP5* and *ACBP6* was not significantly induced by LS (Figure 1b).

The DS- and LS-inducible expression of *ACBP3* was further confirmed by subjecting $ACBP3_{pro}$*:GUS* transgenic lines to dark, DS and LS treatments. Histochemical staining showed that GUS expression in $ACBP3_{pro}$*:GUS* lines was clearly activated by DS and LS (Figure S1).

Altered expression of *ACBP3* changed plant tolerance to submergence

To investigate the role of ACBP3 in hypoxia response, wild-type, *ACBP3-OEs* and *ACBP3-KOs* plants were used to determine their tolerance to hypoxic stress. The growth and development of 4-week-old *ACBP3-OEs* and *ACBP3-KOs* lines was indistinguishable from that of wild type (Figure 2a). When the plant lines were DS-treated for 2 days or LS-treated for 5 days plus a 3-day recovery period, two *ACBP3-OEs* (*OE-1* and *OE-4*) showed increased sensitivity to submergence in comparison with wild type (Figure 2a, d). In contrast, when wild type and *ACBP3-KOs* (*acbp3* and *ACBP3-RNAi*) were treated for 3 days under DS or for 7 days under LS, most *ACBP3-KOs* survived, whereas most wild-type plants died (Figure 2a,d), indicating that depletion of *ACBP3* in *ACBP3-KOs* improved plant tolerance to submergence. The attenuated and enhanced hypoxic tolerance of *ACBP3-OEs* and *ACBP3-KOs*, respectively, was further confirmed by analyses of the survival rates (Figure 2b, e) and dry weights (Figure 2c,f) of DS- or LS-treated plants followed by a 3-day recovery. As shown in Figure 2, both survival rates and dry weights of *ACBP3-OEs* were significantly lower than wild type upon treatment with either 2-day DS or 5-day LS. In contrast, data of both *ACBP3-KOs* were significantly higher than wild type under the extended treatment with 3-day DS or 7-day LS (Figure 2).

Previously, we observed that *ACBP3*-overexpressors showed up-regulation of several defense genes and conferred enhanced resistance to bacterial pathogens (Xiao and Chye, 2011b). To explore whether the differential sensitivities of *ACBP3-OEs* and *ACBP3-KOs* are associated with the expression levels of hypoxia-responsive marker genes, the transcripts of *ADH1*, *PDC1* and *SUS1* were further determined by qRT-PCR in wild-type, *OE-1* and *acbp3* rosettes. As shown in Figure 3, all three transcripts were all significantly induced in wild-type seedlings by DS and LS exposure. Of note, the expression of *ADH1* and *SUS1* at 0, 1, 3 and 6 h, and *SUS1* at 0, 1 and 3 h under DS were significantly down-regulated in *OE-1* in comparison with

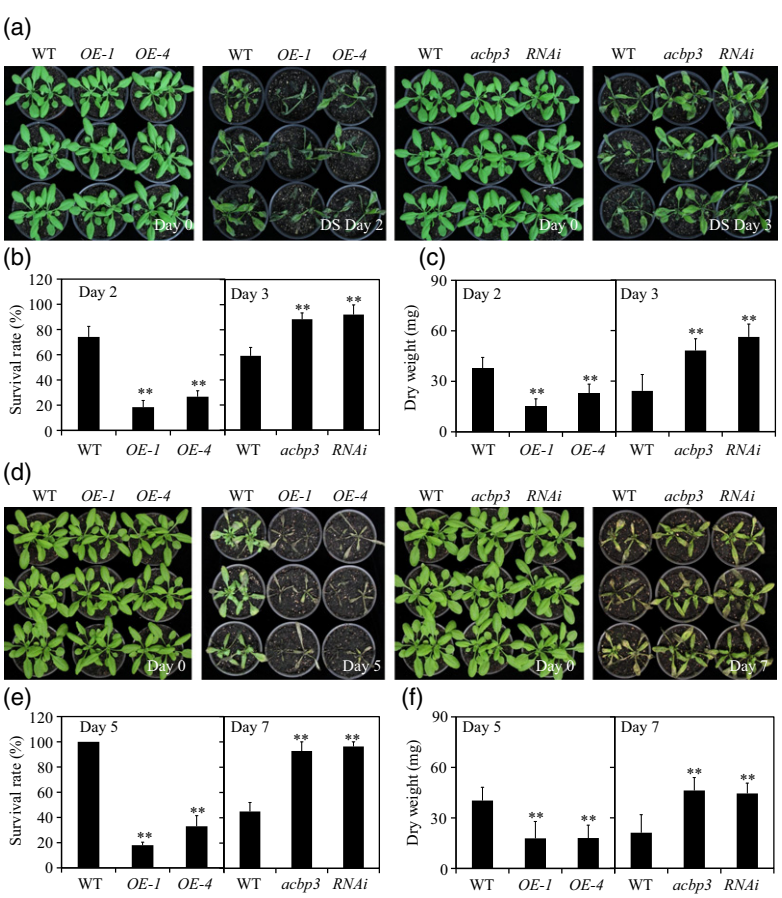

Figure 2. Phenotypes of *ACBP3-OEs* and *ACBP3-KOs* to hypoxic stress.
(a) Phenotypes of 4-week-old wild type (WT), *ACBP3-OEs* (*OE-1* and *OE-4*), *ACBP3-KOs* (*acbp3* and *ACBP3-RNAi*) plants before treatment (day 0) and after 2-day (for *ACBP3-OEs*) or 3-day (for *ACBP3-KOs*) DS treatment, followed by 3 days' recovery.
(b, c) Survival rates (b) and dry weights (c) of WT, *ACBP3-OEs* and *ACBP3-KOs* after DS treatment followed by 3 days' recovery.
(d) Phenotypes of 4-week-old WT, *ACBP3-OEs*, *ACBP3-KOs* before treatment (day 0) and after 5 days (for *ACBP3-OEs*) or 7 days (for *ACBP3-KOs*) of LS treatment, followed by 3 days' recovery.
(e, f) Survival rates (e) and dry weights (f) of the WT, *ACBP3-OEs* and *ACBP3-KOs* after LS treatment followed by 3 days' recovery.
Bars represent means ± SD ($n = 3$) of three independent experiments (for one experiment, >15 plants were scored for each genotype). Asterisks indicate significant differences from WT; $^{**}P < 0.01$ by Student's *t*-test.

wild type (Figure 3a). Similarly, in *OE-1* plants, the expression of all three genes was up-regulated by 3-h LS but down-regulated by 6- and 24-h LS treatments, while the level of *PDC1* was unchanged under 24-h LS (Figure 3b). In contrast, the expression of *ADH1*, *PDC1* and *SUS1* in the *acbp3* mutant showed significant up-regulation following DS and LS treatments at the specific stages, i.e. *ADH1* at 3- and 6-h LS, *PDC1* at 3-h LS and DS, as well as *SUS1* at 6- and 24-h LS (Figure 3). The reduced expression of hypoxia-responsive genes in the *OE-1* line is seemingly correlated with an increased sensitivity to DS and LS stresses.

Accumulation of H_2O_2 in *ACBP3-OEs* under hypoxia

Given *ACBP3-OEs* accumulate high levels of H_2O_2 in rosettes after pathogen infection (Xiao and Chye, 2011b), we tested H_2O_2 levels in *ACBP3-OEs* and *ACBP3-KOs* by diaminobenzidine (DAB) staining upon LS or DS exposure. As shown in Figure 4, both LS (1-, 2- and 3-day) and DS (1-day) treatments triggered the production of H_2O_2, indicated by brown coloration, in wild-type rosettes; however, much higher levels of H_2O_2 were detected in the rosettes of LS- and DS-treated *ACBP3-OEs.* In contrast, the H_2O_2 signals in the rosettes of *ACBP3-KOs* were weaker than wild type at day 2 and day 3 after LS treatment (Figure 4).

The responses of *ACBP3-OEs* and *ACBP3-KOs* to ethanolic treatment

Our preliminary data suggested that exogenous application of ethanol, the end product of anaerobic respiration in plant cells (Bailey-Serres and Voesenek, 2008), could be used to mimic hypoxic stress under certain conditions. To further assess the role of ACBP3 in hypoxia response, wild type, *ACBP3-OEs* and *ACBP3-KOs* were subjected to two types of ethanolic stress. When 4-week-old plants were sprayed with 0.5% ethanol or water (control) and analyzed after 5 days, *ACBP3-OEs* showed greater sensitivity while *ACBP3-KOs* had increased tolerance to ethanol than wild type, as indicated by the extent of yellowing in the rosettes (Figure 5a). Chlorophyll measurements in wild type, *ACBP3-OEs* and *ACBP3-KOs* at 0 and 5 days after ethanol application, confirmed that relative chlorophyll contents had declined significantly in *ACBP3-OEs*, but had increased significantly in *ACBP3-KOs*, compared with wild type after 5 days (Figure 5b). When the seeds of wild type, *ACBP3-OEs* and *ACBP3-KOs* were germinated on Murashige and Skoog (MS) medium supplemented with 0, 50 or 75 mM ethanol for 2 weeks, the *ACBP3-OEs* and *ACBP3-KOs* seedlings displayed less or more ethanol tolerance, respectively, compared with wild type (Figure 5c). Data illustrated that the percentage of *ACBP3-OEs* with true leaves and

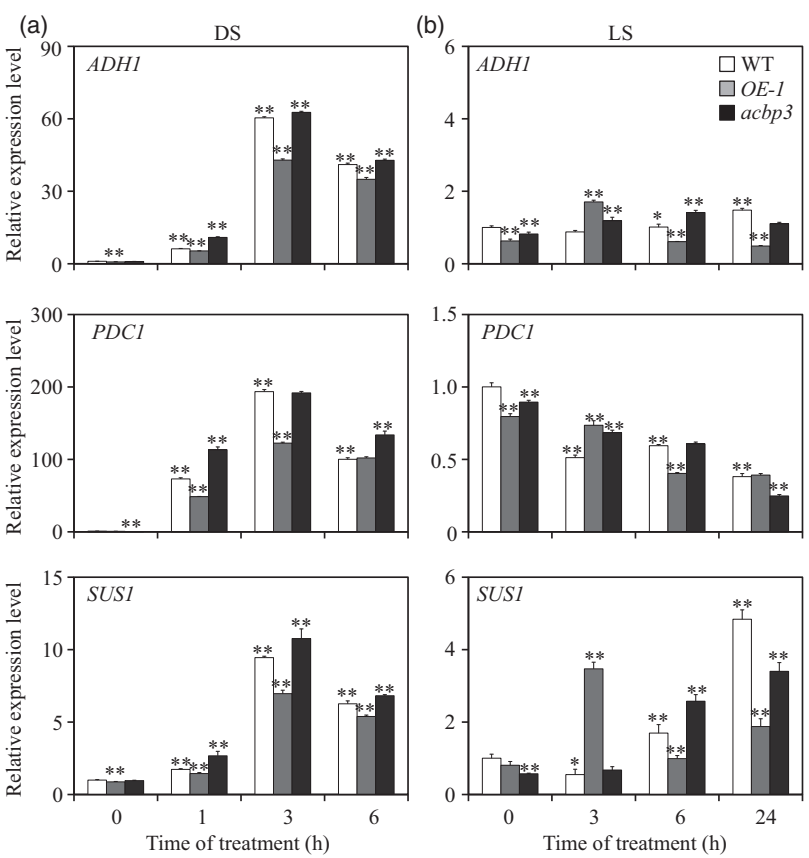

Figure 3. Expression of hypoxia marker genes in *OE-1* and *acbp3* after DS and LS treatments.
Total RNA was isolated from 4-week-old WT, *OE-1* and *acbp3* at 0, 1, 3 and 6 h after DS (a) treatment or 6, 12 and 24 h after LS (b) treatment. Relative expression levels of *ADH1*, *PDC1* and *SUS1* were analyzed by normalizing to a WT sample at 0 h. Data are means ± SD of three independent replicates. Asterisks indicate significant differences from WT; $*P < 0.05$; $**P < 0.01$ by Student's *t*-test. The experiment was repeated with similar results.

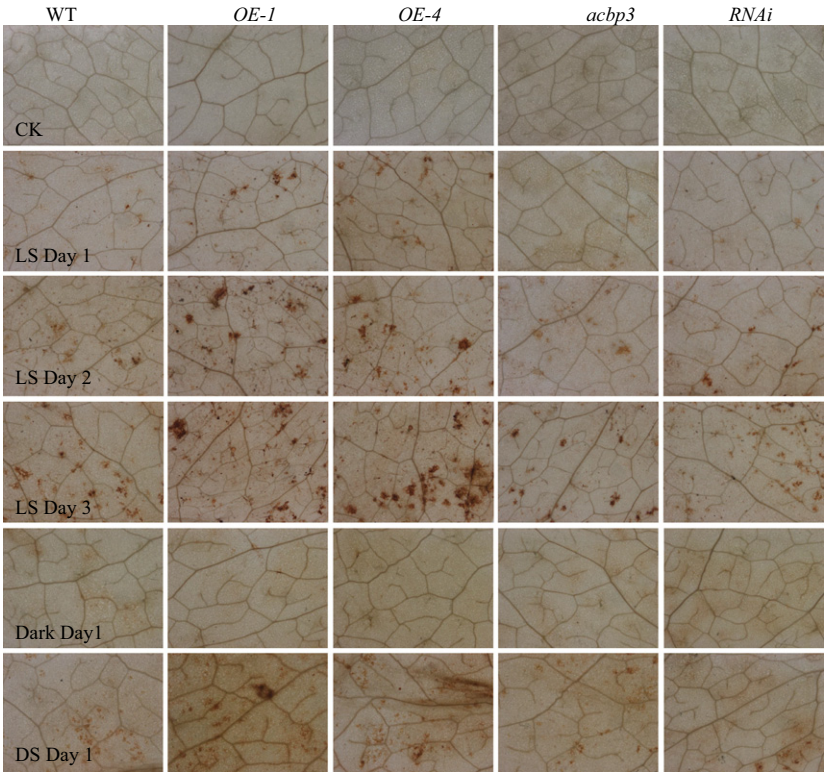

Figure 4. H_2O_2 accumulation in *ACBP3-OEs* and *ACBP3-KOs* upon hypoxic stress.
Rosettes of 4-week-old WT, *ACBP3-OEs* (*OE-1* and *OE-4*), *ACBP3-KOs* (*acbp3* and *ACBP3-RNAi*) before treatment (CK) and after LS (LS day 1, LS day 2 and LS day 3) or DS (DS day 1) treatments were collected and stained by DAB solution.

green cotyledons was significantly lower than wild type on MS medium containing 50 mM ethanol (Figure 5d, upper graph), while that of *ACBP3-KOs* was significantly higher than wild type on MS medium supplemented with 75 mM ethanol (Figure 5d, lower graph).

Hypoxia hypersensitivity in *OE-1* is dependent on NPR1 and CTR1

To investigate whether the hypoxia hypersensitive phenotype in *ACBP3-OE* lines relies on SA or jasmonate (JA)/ethylene (ET) responses, we generated *OE-1 coi1-2*, *OE-1 npr1-5*, and *OE-1 ein3-1* double combinations, which suppressed the SA, JA and ET signaling pathways, respectively. From the phenotypic analyses of single mutants, *npr1-5* plants displayed more tolerance, while the *coi1-2* mutant showed increased sensitivity to both DS and LS, in comparison with wild type (Figure 6a). However, the *ein3-1* mutant was not significantly different to wild type under either DS or LS (Figure 6b), possibly due to the functional redundancy of the *EIL1* gene in Arabidopsis. Interestingly, the hypoxia-sensitive phenotype of *OE-1* was significantly rescued by the *npr1-5* mutation in the *OE-1 npr1-5* double combination (Figure 6a). In contrast, DS and LS treatments revealed that the *OE-1 coi1-2* and *OE-1 ein3-1* double combinations were hypoxia sensitive, resembling the *OE-1* phenotype (Figure 6a,b).

The *OE-1* line was also crossed with the constitutive triple-response mutant *ctr1-1* (Kieber *et al.*, 1993), to generate the *OE-1 ctr1* double combination. Phenotypic analysis showed that upon either DS or LS exposure, the increased hypoxia sensitivity of *OE-1* was partially restored in a *ctr1-1* mutant background (Figure 6c). Together, these results suggest that the hypoxia-sensitive phenotype of *OE-1* is dependent on NPR1 and CTR1, associated with SA and ET signaling, respectively.

Lipid profiling of wild type, *ACBP3-OEs* and *ACBP3-KOs* upon LS exposure

To investigate the potential role of ACBP3 in regulating lipid metabolism during hypoxia, lipid profiles of Arabidopsis rosettes following LS exposure were analyzed. Under normal growth conditions, few differences were detected between wild type and *ACBP3-OEs* or *ACBP3-KOs* except that the levels of phosphatidylserine (PS) increased significantly in *ACBP3-OEs* (Figure 7a). When specific lipid species were analyzed, the levels of C34:3-, C34:2-, C34:1-, C36:5-, C38:3-, C40:3- and C42:3-PS were significantly higher in both *OE-1* and *OE-4* lines compared with wild type (Figure 7b, upper graph). After a 4-day LS treatment, total phosphatidylinositol (PI), PS and phosphatidic acid (PA) levels were significantly elevated in wild-type rosettes, while the levels of other lipids remained unchanged (Figure 7a). In contrast, galactolipids, including digalactosyldiacylglycerol (DGDG) and monogalactosyldiacylglycerol (MGDG), as well as phospholipids such as phosphatidylglycerol (PG), PC, PE and PI, declined in wild-type rosettes

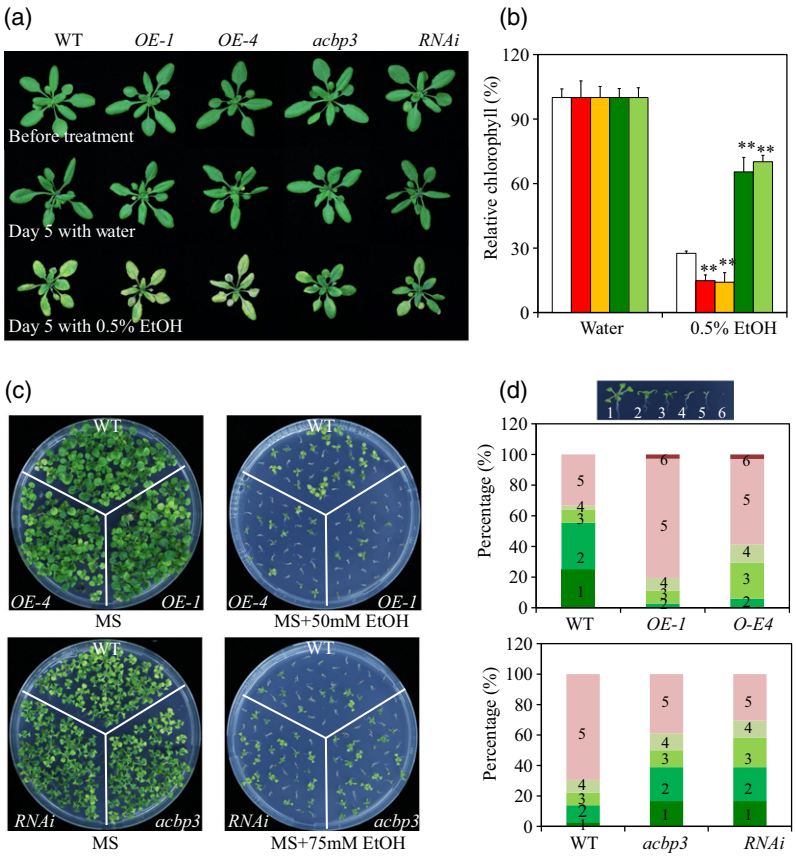

Figure 5. Effects of exogenous ethanol application on *ACBP3-OEs* and *ACBP3-KOs.*
(a) Phenotypes of 4-week-old WT, *ACBP3-OEs* (*OE-1* and *OE-4*) and *ACBP3-KOs* (*acbp3* and *ACBP3-RNAi*) before treatment and at 5 days after spraying with either 0.5% ethanol or water as a control.
(b) Relative chlorophyll contents of plants in (a) treated with ethanol or water control after 5 days. The chlorophyll contents of plants following ethanol treatment were expressed relative to the values of water treatment. Data are average of three samples from three independent plants. Asterisks indicate significant differences to WT; $^{**}P < 0.01$ by Student's *t*-test.
(c) Seeds of WT, *ACBP3-OEs* and *ACBP3-KOs* germinated on MS medium supplemented with 0 (MS), 50 or 75 mM ethanol. Images were taken 2 weeks after germination.
(d) Statistical frequencies of seedlings in (c). The values in the columns correspond to seedlings with true leaves (1 and 2), seedlings with green (3) or brown (4) cotyledons, etiolated seedlings (5), and ungerminated seeds (6).

but PA levels showed significant elevation compared to the untreated control (Figure 7a). In particular, more significant changes were observed in the membrane lipid content between wild-type and *ACBP3-OE* rosettes after LS treatment for 4 days, and between wild-type and *ACBP3-KOs* rosettes after LS treatment for 6 days (Figure 7a). Specifically, total levels of MGDG, DGDG, PG, PC, PI, PS and PA were significantly lower in the rosettes of *ACBP3-OEs* compared to those of wild type under 4-day LS stress, while most of these lipid molecules were remarkably higher in the rosettes of *ACBP3-KOs* than that of 6-day LS-treated wild type (Figure 7a). These data are consistent with increased hypoxia sensitivity in *ACBP3-OEs* but increased tolerance in *ACBP3-KOs.*

Given the significant accumulation of PS in the rosettes of LS-treated wild type and untreated *ACBP3-OEs*, we further analyzed the lipid compositions of different PS species. As shown in Figure 7(b), the levels of unsaturated species such as C36:5-, C36:4-, C36:2-, C38:6-, C38:4-, C38:2-, C40:2-, C42:3-, C42:2- and C44:2-PS declined in both *OE-1* and *OE-4* lines, while those of C34:3-, C34:2-, C36:3-, C36:2-, C38:6-, C38:5-, C38:3-, C38:2-, C40:2-, C42:4-, C42:3-, C42:2-, C44:3- and C44:2-PS increased significantly in *ACBP3-KOs.* Among them, the levels of PS containing VLC species 42:3- and 42:2-PS were the most significantly affected species under LS treatment, which respectively decreased or increased more than two-fold in the rosettes of *ACBP3-OEs* and *ACBP3-KOs* (Figure 7b).

Sphingolipid profile in rosettes of wild type, *ACBP3-OEs* and *ACBP3-KOs* upon hypoxia

Given the significant changes of PS in *ACBP3-OEs* and *ACBP3-KOs* plants exposed to hypoxia, we measured the profiles of the two most abundant sphingolipid species, glucosylinositolphosphorylceramides (GIPCs) and glycosylceramides (GlcCers), as well as the simple ceramides (Cers), in wild type, *ACBP3-OEs* and *ACBP3-KOs* upon LS treatment. Under normal growth conditions, the levels of C22:0-GIPC, C18:0-, C20:0-, C22:0-GlcCer and C16:0-Cer were significantly higher in the *ACBP3-OEs* compared with wild type, but few differences were observed between wild type and *ACBP3-KOs* (Figure 8a–c). Upon 4-day LS exposure, remarkable increases in the levels of most species of GIPCs, GlcCers and Cers were detected in the wild-type rosettes (Figure 8). Compared with the wild-type control, a significant decline in the levels of GIPC classes containing VLCFAs, such as C22:1-, C22:0-, C24:1-, C24:0-, C26:1- and C26:0-GIPC, occurred in *ACBP3-OEs* (Figure 8a). The levels were correspondingly increased in *ACBP3-KOs* after a 6-day LS treatment compared with wild type (Figure 8b).

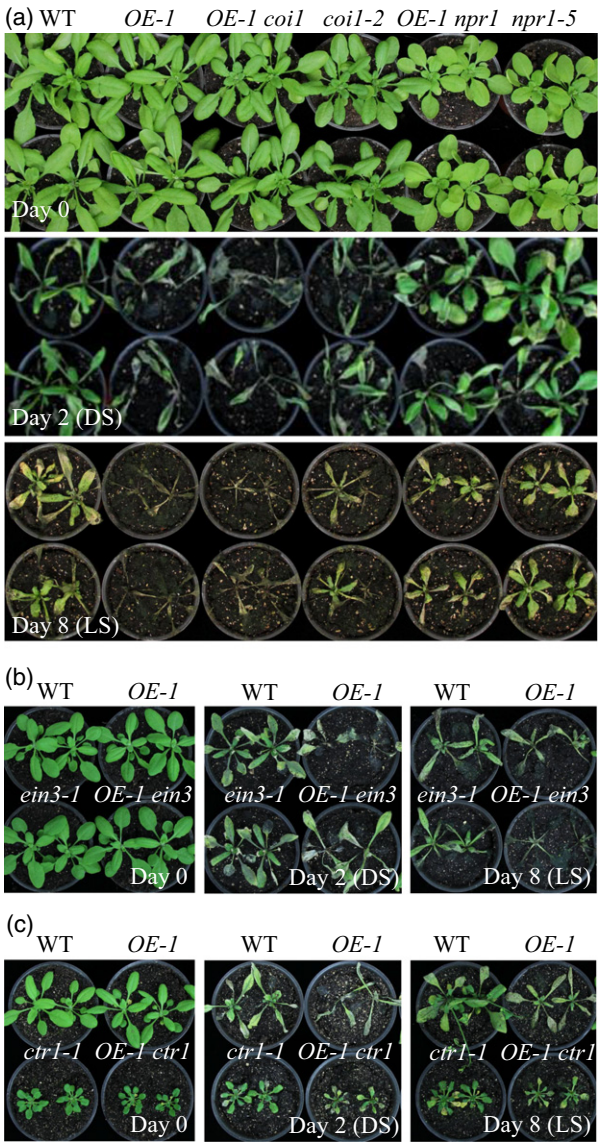

Figure 6. The hypoxia-sensitive phenotype of *OE-1* is dependent on NPR1 and CTR1.
(a) Phenotypes of 4-week-old WT, *OE-1*, *OE-1 coi1*, *coi1-2*, *OE-1 npr1* and *npr1-5* plants before treatment (day 0) and after 2-day DS or 8-day LS treatment followed by 3 days recovery.
(b, c) Phenotypes of 4-week-old WT, *OE-1*, *ein3-1*, *OE-1 ein3* (b), and *ctr1-1* and *OE-1 ctr1* (c) plants before (day 0) and after 2-day DS or 8-day LS treatment followed by 3 days recovery.

No significant changes in the compositions of GlcCer were detected in any of the three genotypes upon LS exposure. In contrast, significant decreases of C22:1- and C24:1-Cer were detected in LS-treated *OE-1* (Figure 8c). However, the levels of C16:0-Cer varied significantly, increasing 4.9-fold in the *OE-1* and declining 2.3-fold in the *acbp3* mutant in comparison with wild type after LS treatment (Figure 8c).

ACBP3 recombinant protein binds VLC-acyl-CoAs *in vitro*

The binding of rACBP3 to 20:4-CoA esters (Leung *et al.*, 2006) may represent its ability to target VLC acyl-CoAs. To address this possibility, the rACBP3 protein was expressed and purified from *Escherichia coli* and its binding affinities to different VLC acyl-CoAs were determined by microscale thermophoresis (MST) analysis, which is a sensitive approach to measure protein-ligand interactions *in vitro.* Data presented in Figure 9 show that the dissociation constant (K_d) of rACBP3-18:2-CoA interaction was 0.788 μM in MST measurement, which is comparable with that of Lipidex assay (Xiao *et al.*, 2010). Moreover, we found that rACBP3 bound VLC acyl-CoAs including 20:0-, 22:0- and 24:0-CoA with higher affinities than observed for 18:2-CoA, as reflected by the K_d values at nmol levels (Figure 9). These results indicate that ACBP3 preferentially binds VLC acyl-CoAs *in vitro.*

The VLCFA-mediated hypoxia response is controlled by MYB30

The transcription factor MYB30 serves as a key regulator of VLCFA metabolism by regulating various genes encoding subunits of the acyl-CoA elongase complex (Raffaele *et al.*, 2008). To evaluate the role of MYB30 in the potential regulation of hypoxia-induced VLCFA metabolism, the *MYB30* knockout mutant *myb30-1* (Zheng *et al.*, 2012b) was obtained and the *ACBP3-RNAi myb30* double combination was generated. As shown in Figure 10, the *myb30-1* single mutant displayed hypersensitivity to both LS (Figure 10a) and ethanol (Figure 10b) treatments, indicating that MYB30 plays an essential role in moderating the hypoxia response. In contrast, the *ACBP3-RNAi myb30* plants showed enhanced tolerance to both LS and ethanolic stresses, similar to that of the *ACBP3-RNAi* phenotype (Figure 10). These results, together with lipid profiling data showing increased accumulation of VLCFA-containing PS and GIPC in *ACBP3-RNAi*, suggest that ACBP3 acts downstream of MYB30 in VLCFA-mediated hypoxia signaling.

DISCUSSION

We have previously demonstrated that Arabidopsis ACBP3 is crucial for the promotion of leaf senescence and plant resistance to hemi-biotrophic pathogens (Xiao *et al.*, 2010; Xiao and Chye, 2011b). Here, we present several lines of evidence to support a role for ACBP3 in the modulation of hypoxic tolerance, which is associated with the cellular homeostasis of VLCFA metabolism. First, rACBP3 protein bound to VLC acyl-CoA esters with high affinities. Second, LS triggered a significant accumulation of VLC-enriched PS and GIPC compounds in rosettes, whose levels remarkably declined or increased in *ACBP3-OEs* and *ACBP3-KOs*, respectively, upon LS exposure. Third, deletion of Arabidopsis MYB30, the master regulator of VLCFA biosynthesis

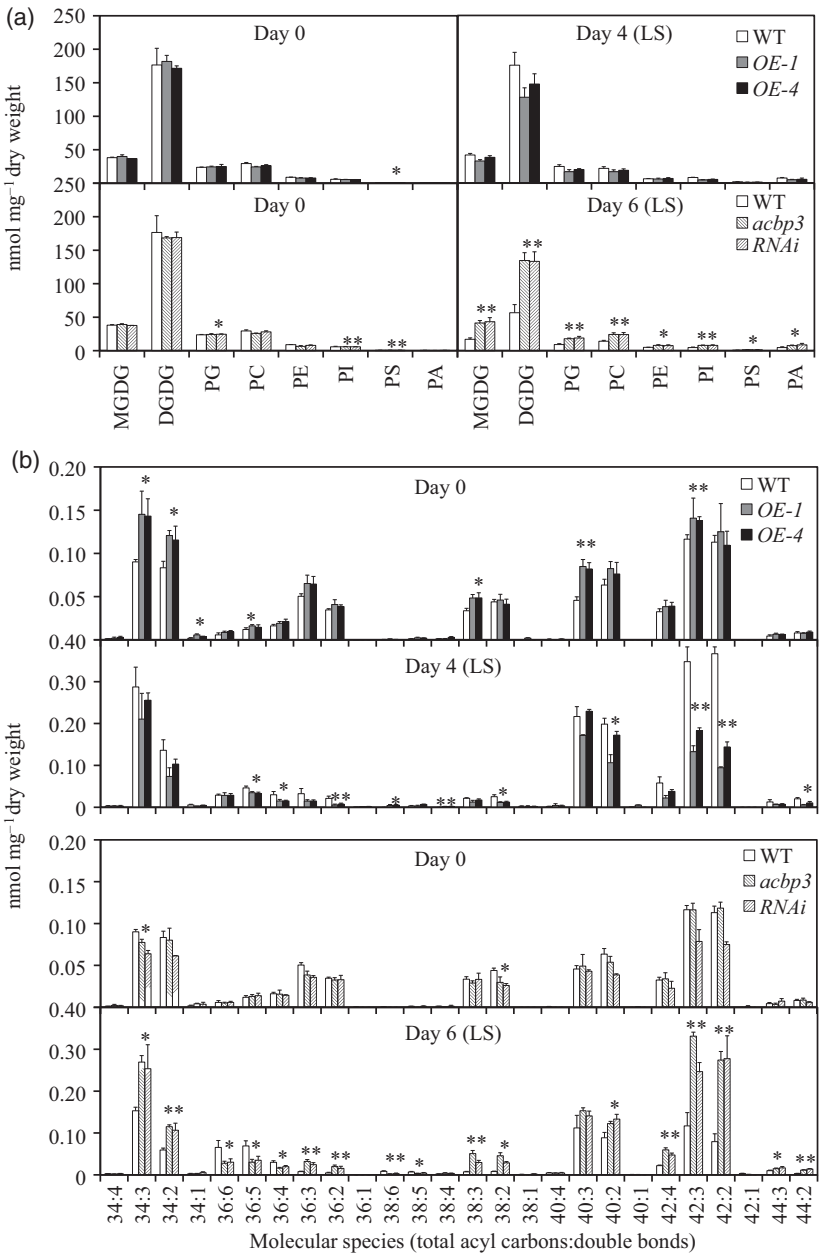

Figure 7. Lipid profiles in the rosettes of WT, *ACBP3-OEs* and *ACBP3-KOs* after LS treatment.
(a) Content of lipid species of 4-week-old WT, *ACBP3-OEs* (*OE-1* and *OE-4*) and *ACBP3-KOs* (*acbp3* and *ACBP3-RNAi*) before treatment (day 0) and after LS treatment for 4 days (LS day 4; for *ACBP3-OEs*) or 6 days (LS day 6; for *ACBP3-KOs*).
MGDG, monogalactosyldiacylglycerol; DGDG, digalactosyldiacylglycerol; PG, phosphatidylglycerol; PC, phosphatidylcholine; PE, phosphatidylethanolamine; PI, phosphatidylinositol; PS, phosphatidylserine; PA, phosphatidic acid.
(b) Lipid compositions of PS in WT and *ACBP3-OEs* before treatment (day 0) or after 4-day LS treatment (upper two graphs), and WT and *ACBP3-KOs* before treatment (day 0) or after 6-day LS treatment (lower two graphs).
Asterisks indicate significant differences from WT; $*P < 0.05$; $**P < 0.01$ by Student's *t*-test. Values represent means ± SD ($n = 4$) of four independent samples and each sample was pooled from the rosettes of three plants.

in response to pathogen attack (Raffaele *et al.*, 2008), attenuated plant sensitivity to LS and ethanolic stresses. Moreover, *ACBP3-RNAi* ameliorated the *myb30-1* hypoxia-sensitive phenotype. Therefore, our findings demonstrate a mechanism for the involvement of VLCFAs or VLCFA-derivatives in plant response to hypoxia.

In higher plants, most of the plastidial C16:0- and C18:0-fatty acyl-CoAs are exported to the endoplasmic reticulum (ER) membrane for either biosynthesis of membrane lipids by ER-resident enzymes, or assembly of VLCFAs by the fatty acid elongase complex (Ohlrogge and Browse, 1995; Li-Beisson *et al.*, 2013). By their binding ability to differential acyl-CoA esters, ACBPs are primarily deemed to maintain acyl-CoA pools and modulate lipid biosynthesis *in vivo* (Fan *et al.*, 2010; Xiao and Chye, 2011a). Besides, ACBPs can also function in the delivery of acyl-CoAs to enzymes such as lysophosphatidic acid acyltransferase and glycerol-3-phosphate acyltransferase, both of which require acyl-CoAs as substrates for lipid biogenesis (Xiao and Chye, 2011a).

In this study, MST analysis showed that rACBP3 binds not only LC acyl-CoA esters (C18-CoA), which is consistent with previous findings (Leung *et al.*, 2006; Xiao *et al.*, 2010), but also to VLC acyl-CoA esters (C20:0-, C22:0- and C24:0-CoAs) with higher affinities (Figure 9). This suggests that rACBP3 is able to interact with C18-CoA and VLC

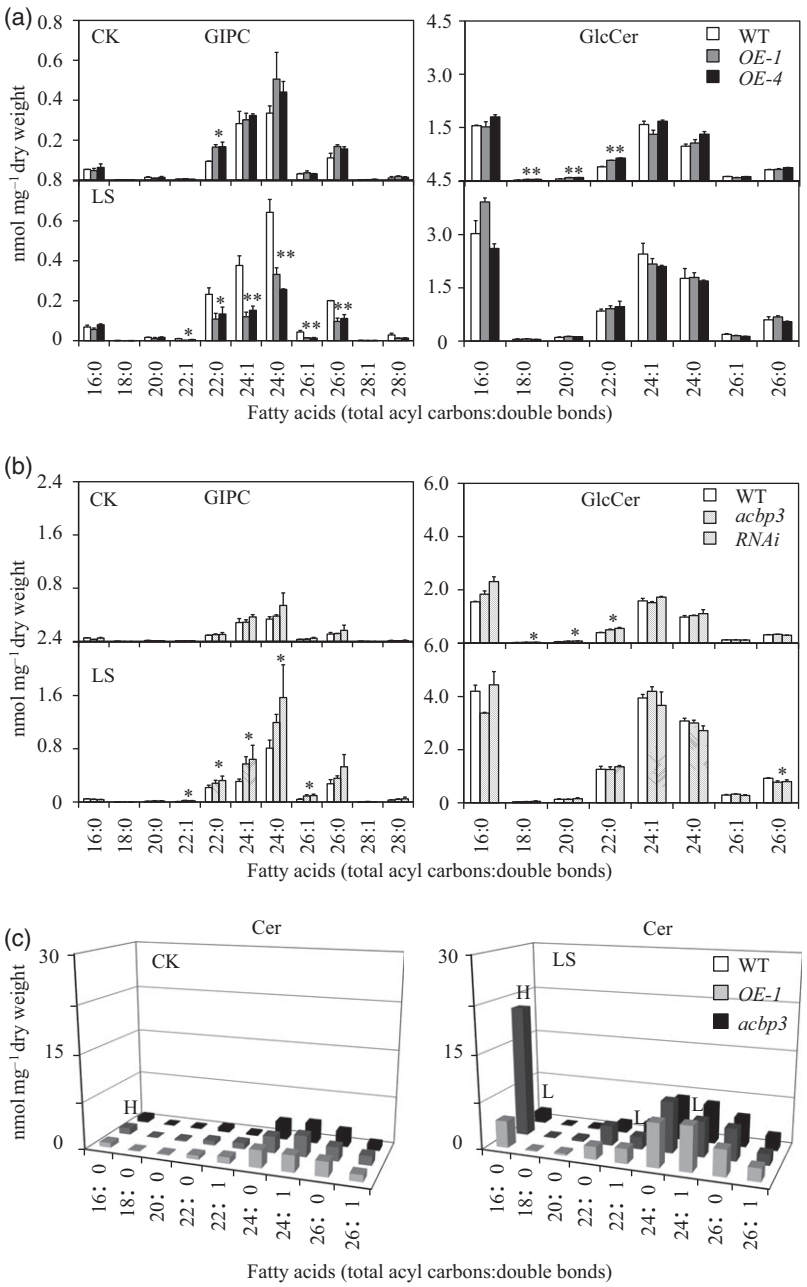

Figure 8. Sphingolipid contents in rosettes of WT, *ACBP3-OEs* and *ACBP3-KOs* after LS treatment.

For GIPC and GlcCer profiling, 4-week-old WT, *ACBP3-OEs* (*OE-1* and *OE-4*) and *ACBP3-KOs* (*acbp3* and *ACBP3-RNAi*) were untreated (CK), LS-treated for 4 days (a; for *ACBP3-OEs*), or LS-treated for 6 days (b; for *ACBP3-KOs*). For ceramide profiling, 4-week-old WT, *OE-1* and *acbp3* plants were untreated (CK) or LS-treated for 2 days (LS). The rosette samples were harvested at the indicated times. The amounts of GIPC (left panels in a, b), GlcCer (right panels in a, b) and Cer (c) were calculated by normalizing to the dry weights of tissues.

Asterisks indicate significant differences from WT; $*P < 0.05$; $**P < 0.01$ by Student's *t*-test. Values represent means ± SD ($n = 4$) of four independent samples and each sample was pooled from the rosettes of three plants.

acyl-CoA esters, and deliver them as potential substrates for lipid metabolism. In agreement with this result, a study using isothermal titration calorimetry (ITC) revealed that rACBP1 could also bind VLC acyl-CoA *in vitro* (Xue *et al.*, 2014). Furthermore, investigations using T-DNA insertion mutants by two independent groups have recently demonstrated that depletion of either ACBP1 or ACBP3 impaired cuticle development in Arabidopsis stems and leaves, respectively (Xia *et al.*, 2012; Xue *et al.*, 2014). Thus, it is conceivable that Arabidopsis ACBP1 and ACBP3 play crucial roles in cuticle formation, possibly by shuttling VLC acyl-CoAs to elongases, and thereby influencing the subsequent cuticular lipid biosynthesis.

In addition to cuticular lipids, VLCFAs are known to be precursors for synthesis of sphingolipids, which originate in the ER by condensation of serine and palmitoyl-CoA to produce 3-ketosphinganine (Lynch and Dunn, 2004; Chen *et al.*, 2009; Li-Beisson *et al.*, 2013). Ceramides are assembled by acylating sphinganine to an acyl-CoA molecule and, in turn, serve as direct substrates for the generation of complex sphingolipids such as GlcCers and GIPCs, which are enriched in C16-fatty acids and VLCFAs,

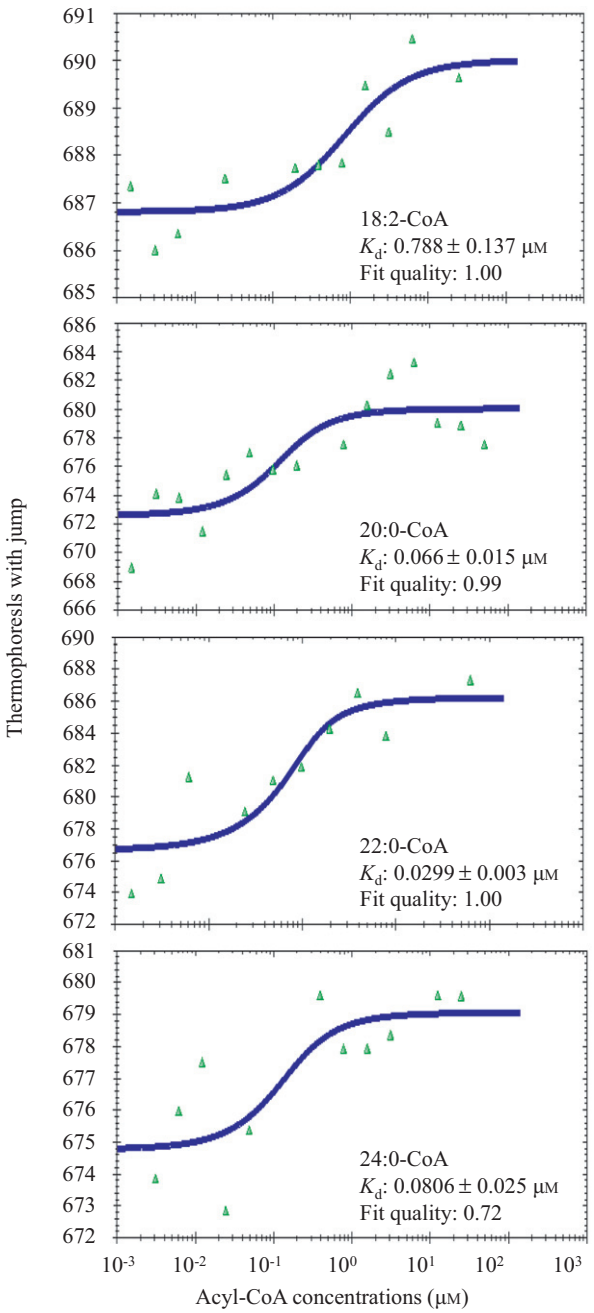

Figure 9. rACBP3 protein binds VLC acyl-CoA esters *in vitro*.
The interactions between rACBP3 and 18:2-, 20:0-, 22:0- and 24:0-acyl-CoA esters were determined by MST analyses. The dissociation constant (K_d) calculated for each binding assay is shown.

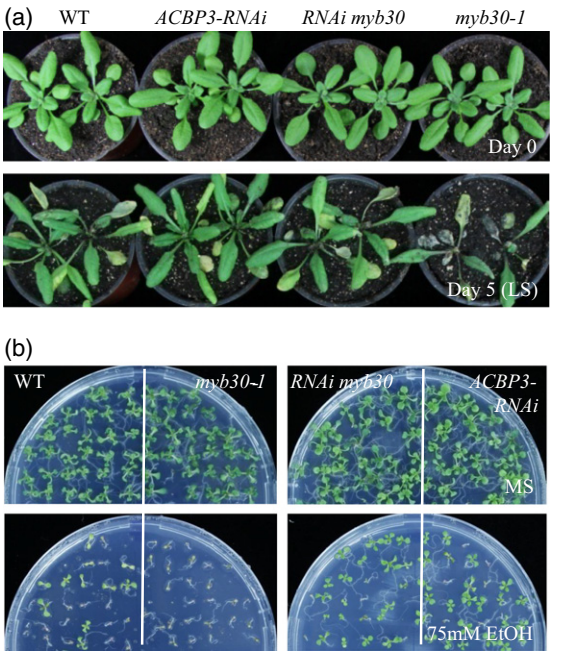

Figure 10. Regulation of ACBP3-mediated hypoxia response by MYB30.
(a) Phenotypes of 4-week-old WT, *ACBP3-RNAi*, *RNAi myb30*, and *myb30-1* plants before treatment (day 0) and after 5-day LS treatment followed by 3 days' recovery.
(b) Seeds of WT, *ACBP3-RNAi*, *RNAi myb30*, and *myb30-1* were germinated on MS medium supplemented with 0 (MS) or 75 mM ethanol. Images were taken 2 weeks after germination.

respectively (Lynch and Dunn, 2004; Chen *et al.*, 2009; Li-Beisson *et al.*, 2013). Our lipidomic data further extend the significance of ACBP3 in modulating the biosynthesis of sphingolipids, particularly the classes of VLCFA-enriched GIPCs in Arabidopsis. The effect of ACBP3 in modulating the composition of sphingolipids resembles that of yeast ACBP (ACB1), whose depletion in *Saccharomyces cerevisiae* led to dramatic reductions of C26:0-VLCFA and sphingolipids by 50–70% (Gaigg *et al.*, 2001). However, evidence that yeast ACB1 binds to C16:0-CoA, but not VLC acyl-CoAs, suggests that ACB1 may function in yeast sphingolipid biosynthesis by shuttling and incorporating C16:0-CoA into d18:0 sphinganine for the production of LC-ceramides (Gaigg *et al.*, 2001). Given that rACBP3 did not bind to C16:0-CoA (Leung *et al.*, 2006), it may therefore function in the sphingolipid pathway in plants through a different way to that of yeast. Instead, its high affinity to VLC acyl-CoAs may contribute to controlling the incorporation of VLC acyl-CoAs into t18:0 sphinganine for production of VLC-ceramides as well as GIPCs. In agreement with this proposal, we observed that under normal growth conditions, the levels of C22:0-GIPC and C20:0- and C22:0-GlcCers were significantly increased in the *ACBP3-OEs* in comparison with wild type (Figure 8). In contrast, upon LS exposure, a significant decline in VLC-GIPCs (C22:0, C22:1, C24:0, C24:1, C26:0 and C26:1) was detected in the *ACBP3-OEs*, and vice versa in *ACBP3-KOs* (Figure 8), indicating that VLC-GIPCs are essential for activation of hypoxia response and for protecting Arabidopsis from hypoxic stress. Interestingly, we also observed that the levels of C16:0-Cer showed contrasting accumulation patterns in LS-treated *ACBP3-OEs* and *ACBP3-KOs*, with high accumulation occurring in *ACBP3-OEs* but a decline occurring in

ACBP3-KOs. The corresponding cell death phenotypes (Xiao and Chye, 2011b) and C16:0-Cer accumulation in *ACBP3-OEs* resembled the knockout mutant phenotype corresponding to LOH1, a ceramide synthase responsible for synthesis of VLC-Cers in Arabidopsis (Markham *et al.*, 2011; Ternes *et al.*, 2011), further confirming the potential function of ACBP3 in VLC-sphingolipid biogenesis.

The transcription factor MYB30 is a positive regulator in the activation of hypersensitive cell death (Vailleau *et al.*, 2002) and abscisic acid response (Zheng *et al.*, 2012b). MYB30 regulates genes encoding key components of the acyl-CoA elongase complex, and changes to *MYB30* expression greatly influence accumulation patterns of VLCFAs as well as VLCFA-derived metabolites including leaf wax and sphingolipids (Raffaele *et al.*, 2008). This suggests that MYB30 is an upstream master regulator for the stress-triggered production of VLCFAs. Consistent with this proposal, our phenotypic data obtained from analyzing the responses of *myb30-1* to submergence and ethanolic treatments, indicate that MYB30 is required for hypoxia response (Figure 10), and provides validation of our biochemical data. Many reports on plant defense signaling have revealed that VLCFAs and their derivatives GIPCs are essential components for mediating the SA response (Raffaele *et al.*, 2008; Wang *et al.*, 2008; Mortimer *et al.*, 2013). For example, two Arabidopsis mutants *erh1* and *gonst1* that lack the inositolphosphorylceramide synthase and the GDP-D-mannose transporter, respectively, have severely reduced GIPCs as well as SA-mediated programmed cell death in rosettes (Wang *et al.*, 2008; Mortimer *et al.*, 2013). Similarly, the SA dependence of ACBP3 in both plant defense and hypoxia responses has been established previously (Xiao and Chye, 2011b) and confirmed in the present study (Figure 6) by phenotypic analyses of the *OE-1 npr1-5* double combination. Nonetheless, observations that defense signaling mutants such as *npr1-5*, *coi1-2*, *ein3-1* and *ctr1-1* of the SA and JA/ET pathways showed altered tolerance to hypoxia (Figure 6) suggest a link between the defense and hypoxia signaling pathways. Moreover, a recent investigation demonstrated that submergence strongly induces the transcription of a large number of defense genes in Arabidopsis (Hsu *et al.*, 2013). By targeting genes involved in plant innate immunity, the transcription factor WRKY22 was shown to be a key regulator in protecting plants against pathogen infection during or after submergence (Hsu *et al.*, 2013). Further investigations that determine how defense hormones control the plant response to hypoxic stress are required in order to deepen our understanding of the interaction between hypoxia and defense signaling.

Finally, we would like to propose the potential mechanism of ACBP3, VLCFAs and their derivatives in the plant response to hypoxia. Our results illustrate that the sensitivities of *ACBP3-OEs* and *ACBP3-KOs* to hypoxic stress were negatively correlated with the rosette H_2O_2 levels (Figure 4). The hypoxia-induced accumulation of H_2O_2 in *ACBP3-OEs* is consistent with the compositional alterations of Cer species in these lines (Figures 7 and 8), whose abnormal changes severely affect the SA-dependent H_2O_2 production in plant cells (Raffaele *et al.*, 2008; Mortimer *et al.*, 2013). In general, low levels of H_2O_2 act as an essential second messenger to transmit initial signals to activate plant stress responses. However, excessive accumulation of H_2O_2 can result in irreversible oxidative damages to cellular components and eventually lead to cell death (Apel and Hirt, 2004). Recent studies have also highlighted a direct link between hypoxia/anoxia responses and ROS signaling (Baxter-Burrell *et al.*, 2002; Pucciariello *et al.*, 2012; Yang, 2014). Particularly, the ROP-triggered elevation of H_2O_2 levels under anoxia was accompanied with an increase in the activity of ADH1 and enhanced plant tolerance to oxygen deprivation (Baxter-Burrell *et al.*, 2002). Thus, it is most likely that the hypoxia-activation of *ACBP3*, VLCFAs as well as VLCFA-derivatives may enhance plant survival during hypoxic stress by modulating the cellular homeostasis of ROS. However, the over-production of H_2O_2 in the rosettes of *ACBP3-OEs* may contribute to the hypersensitivity to hypoxia observed here. Whereas in the *ACBP3-KO* lines, the moderate levels of H_2O_2 appear to improve plant tolerance to submergence.

EXPERIMENTAL PROCEDURES

Plant materials and growth conditions

Wild-type Arabidopsis used in this study was Columbia ecotype (Col-0). Characterizations of *ACBP3-OEs* (*OE-1* and *OE-4*) and *ACBP3-KOs* (*acbp3* and *ACBP3-RNAi*) and *ACBP3*$_{pro}$*:GUS* lines have been previously described (Xiao *et al.*, 2010; Zheng *et al.*, 2012a). The double combinations of *OE-1 coi1* and *OE-1 npr1* were generated following Xiao *et al.* (2010). *OE-1 ein3* and *OE-1 ctr1* combinations were generated by crossing *OE-1* with *ein3-1* (Chao *et al.*, 1997) and *ctr1-1* (Kieber *et al.*, 1993). *ACBP3-RNAi myb30* was generated by crossing *ACBP3-RNAi* with *myb30-1* (SALK_122884; Zheng *et al.*, 2012b). Seedlings displaying insensitivity to ethylene (Chao *et al.*, 1997) and constitutive triple-response phenotypes (Kieber *et al.*, 1993) were deemed to be homozygous for *ein3-1* and *ctr1-1*, respectively. The T-DNA insertion in the *myb30-1* line was identified by PCR (Zheng *et al.*, 2012b).

All Arabidopsis seeds were surface-sterilized with 20% bleach containing 0.1% Tween-20 for 20 min, and then washed five times with sterile water. Seeds were sown on MS medium (Murashige and Skoog, 1962), followed by cold treatment for 3 days. After germination for 7 days, seedlings were transplanted to soil and grown in a plant growth room under 16-h light/8-h dark cycle at 22°C.

Hypoxic treatments

Hypoxic treatments were carried out following Licausi *et al.* (2011a). Briefly, 4-week-old plants were submerged under LS and DS or darkness as a control. Rosettes were submerged 10 cm

below the water surface. Plant samples were collected or photographed at the indicated times. Survival rates and dry weights were scored after treatment following recovery for 3 days. Data presented in this study are means ± standard deviation (SD) (n = 3) of three independent experiments (for one experiment, >15 plants were scored for each genotype).

For ethanolic spraying assays, 4-week-old plants were sprayed with 0.5% (v/v) ethanol and covered to maintain high humidity for 5 days. Samples were collected after treatment and chlorophyll contents were measured according to Xiao *et al.* (2010). For germination assays, surface-sterilized seeds were sown on MS solid medium with 0, 50 or 75 mM ethanol, followed by cold treatment for 2 days, and grown under normal growth conditions for 2 weeks. The experiment was repeated with similar results.

RNA extraction and qRT-PCR analysis

RNA extraction and qRT-PCR analysis were performed as described previously (Xiao and Chye, 2011b). The isolated RNA was reverse transcribed using the PrimeScript™ RT reagent Kit (TaKaRa, http://www.takara-bio.com/) following the manufacturer's instructions. qRT-PCR was analyzed using SYBR Green master mix (TaKaRa) on a StepOne Plus real-time PCR system (Applied Biosystems, http://www.appliedbiosystems.com/). The conditions for qRT-PCR were initial denaturation at 95°C for 5 min followed by 40 cycles of PCR (denaturing, 95°C for 10 sec; annealing, 55°C for 15 sec; extension, 72°C for 30 sec). Three experimental replicates were used for each reaction. The *ACTIN2* gene was used as reference gene. Gene-specific primers used for qRT-PCR analysis are listed in Table S1.

DAB staining

DAB staining was performed as described previously (Xiao and Chye, 2011b). Rosettes were excised and placed in 1 mg ml^{-1} DAB staining solution (pH 3.8) for 3 h at room temperature under darkness and subsequently cleared in 96% boiling ethanol for 10 min. After cooling, the leaves were retained in ethanol and photographed.

Measurements of polar membrane lipids and sphingolipids

For membrane lipid analysis, the total plant lipids were extracted following Welti *et al.* (2002). The profiles of membrane lipids were determined by electrospray ionization–tandem mass spectrometry (ESI-MS/MS) as previously described (Devaiah *et al.*, 2006; Xiao *et al.*, 2010). Data showed in this study are means ± SD of four independent samples and each sample was pooled from the rosettes of three plants.

Extraction of sphingolipids was carried out according to Markham *et al.* (2006) using 100 mg tissue samples. Briefly, an 8-ml isopropanol/n-hexane/water solvent (50/20/25; v/v/v) was added to the freeze-dried samples, and the mixture was fully homogenized using a glass homogenizer. The extract was transferred to a glass tube, and C17 LCB, C12 Ceramide, C12 glucosylceramide (Avanti, http://www.avantilipids.com/) were added as internal standards, followed by incubation at 60°C for 15 min with occasional shaking. After centrifuging at 1000 ***g*** for 10 min, the supernatant was transferred to a fresh tube and the pellet was extracted twice more. The combined supernatants were subsequently evaporated under nitrogen and de-esterified in 33% methylamine in ethanol/water (7:3; v/v) followed by a 1-h incubation at 50°C (Markham and Jaworski, 2007).

The extracts were dried under nitrogen, then dissolved in 1 ml of methanol and analyzed on a triple TOF 5600 MS/MS system (AB SCIEX, http://www.absciex.com/, Canada). Separations were accomplished on an Agilent Eclipse XDB C8 column (50 × 2.1 mm, 1.8 μm) (Agilent, http://www.agilent.com/). The column heater temperature was maintained at 40°C. The mobile phases were composed of 100% methanol and 1 mM ammonium formate with 0.2% formic acid and the flow rate was 0.3 ml min^{-1}. The sample volume injected was 10 μl. The MS/MS detector parameters were set as follows: temperature 450°C; curtain gas 30 psi; flow rate 10 L min^{-1}; and ion spray voltage 5000 V. Quantification was performed based on peak area and internal standards (Markham and Jaworski, 2007).

MST binding assay

For MST binding analysis, rACBP3 protein samples were first labeled with the Monolith NT™ Protein Labeling Kit RED (http://www.nanotemper-technologies.com/). Labeled protein was used at a concentration of 10 nM in 1× phosphate buffered saline (pH 7.6) containing 0.05% Tween-20. The concentration of various acyl-CoA esters (Avanti) ranged from 1.5 nM to 50 μM. An optimized buffer (50 mM Tris–HCl pH 7.4, 150 mM NaCl, 10 mM $MgCl_2$, 0.05% Tween-20) was prepared for incubation of rACBP3 and acyl-CoA esters for 5 min. The combined solution of labeled protein and acyl-CoA esters was transferred into standard treated capillaries and MST was measured on a NanoTemper Monolith NT.115 (20% LED power; 50% laser power).

ACKNOWLEDGEMENTS

We thank the ABRC for provision of *ein3-1*, *ctr1-1* and *npr1-5* mutant seeds, Y. Guo (Chinese Agricultural University) for *myb30-1* seeds, D.X. Xie (Tsinghua University) for the *coi1-2* seeds and M. L. Chye (University of Hong Kong) for the *ACBP3-OEs*, *ACBP3-KOs* and *$ACBP3_{pro}$:GUS* lines. We also thank M. Roth and R. Welti (Kansas Lipidomics Research Center, USA) for membrane lipid profiling. This work was supported by the National Natural Science Foundation of China (Projects 31461143001, 31370298 and 31200200), Program for New Century Excellent Talents in University (Project NCET-13-0614), the Key Project of Department of Education of Guangdong Province (Project 2012CXZD0003), the Fundamental Research Funds for the Central Universities (Project 12lgzd02) and Sun Yat-sen University (Start-up fund to S.X.).

SUPPORTING INFORMATION

Additional Supporting Information may be found in the online version of this article.

Figure S1. Expression patterns of *$ACBP3_{pro}$:GUS* upon DS and LS treatments.

Table S1. Sequence of gene-specific primers used for qRT-PCR.

REFERENCES

Apel, K. and Hirt, H. (2004) Reactive oxygen species: metabolism, oxidative stress, and signal transduction. *Annu. Rev. Plant Biol.* **55**, 373–399.

Bailey-Serres, J. and Voesenek, L.A.C.J. (2008) Flooding stress: acclimations and genetic diversity. *Annu. Rev. Plant Biol.* **59**, 313–339.

Bailey-Serres, J. and Voesenek, L.A.C.J. (2010) Life in the balance: a signaling network controlling survival of flooding. *Curr. Opin. Plant Biol.* **13**, 489–494.

Bailey-Serres, J., Fukao, T., Gibbs, D.J., Holdsworth, M.J., Lee, S.C., Licausi, F., Perata, P., Voesenek, L.A.C.J. and van Dongen, J.T. (2012) Making sense of low oxygen sensing. *Trends Plant Sci.* **17**, 129–138.

Baxter-Burrell, A., Yang, Z., Springer, P.S. and Bailey-Serres, J. (2002) RopGAP4-dependent Rop GTPase rheostat control of Arabidopsis oxygen deprivation tolerance. *Science*, **296**, 2026–2028.

Burton, M., Rose, T.M., Faergeman, N.J. and Knudsen, J. (2005) Evolution of the acyl-CoA binding protein (ACBP). *Biochem. J.* **392**, 299–307.

Chang, W.W., Huang, L., Shen, M., Webster, C., Burlingame, A.L. and Roberts, J.K. (2000) Patterns of protein synthesis and tolerance of anoxia in root tips of maize seedlings acclimated to a low-oxygen environment, and identification of proteins by mass spectrometry. *Plant Physiol.* **122**, 295–318.

Chao, Q., Rothenberg, M., Solano, R., Roman, G., Terzaghi, W. and Ecker, J.R. (1997) Activation of the ethylene gas response pathway in Arabidopsis by the nuclear protein ETHYLENE-INSENSITIVE3 and related proteins. *Cell*, **89**, 1133–1144.

Chen, Q.F., Xiao, S. and Chye, M.L. (2008) Overexpression of the Arabidopsis 10-kilodalton acyl-coenzyme A-binding protein ACBP6 enhances freezing tolerance. *Plant Physiol.* **148**, 304–315.

Chen, M., Saucedo-García, M., Gavilanes-Ruíz, M., Plascencia, J. and Cahoon, E. B. (2009) Plant sphingolipids: structure, synthesis and function. In *Lipids in Photosynthesis: Essential and Regulatory Functions, Advances in Photosynthesis and Respiration* (Wada, H. and Murata, N., ed). Dordrecht: Springer, pp. 77–115.

Devaiah, S.P., Roth, M.R., Baughman, E., Li, M., Tamura, P., Jeannotte, R., Welti, R. and Wang, X. (2006) Quantitative profiling of polar glycerolipid species from organs of wild type Arabidopsis and a *PHOSPHOLIPASE Dα1* knockout mutant. *Phytochemistry*, **67**, 1907–1924.

Du, Z.Y. and Chye, M.L. (2013) Interactions between Arabidopsis acyl-CoA-binding proteins and their protein partners. *Planta*, **238**, 239–245.

Du, Z.Y., Chen, M.X., Chen, Q.F., Xiao, S. and Chye, M.L. (2013) Arabidopsis acyl-CoA-binding protein ACBP1 participates in the regulation of seed germination and seedling development. *Plant J.* **74**, 294–309.

Fan, J., Liu, J., Culty, M. and Papadopoulos, V. (2010) Acyl-coenzyme A binding domain containing 3 (ACBD3; PAP7; GCP60): an emerging signaling molecule. *Prog. Lipid Res.* **49**, 218–234.

Gaigg, B., Neergaard, T.B., Schneiter, R. *et al.* (2001) Depletion of acyl-coenzyme A-binding protein affects sphingolipid synthesis and causes vesicle accumulation and membrane defects in *Saccharomyces cerevisiae*. *Mol. Biol. Cell*, **12**, 1147–1160.

Gao, W., Xiao, S., Li, H.Y., Tsao, S.W. and Chye, M.L. (2009) *Arabidopsis thaliana* acyl-CoA-binding protein ACBP2 interacts with heavy-metal-binding farnesylated protein AtFP6. *New Phytol.* **181**, 89–102.

Gao, W., Li, H.Y., Xiao, S. and Chye, M.L. (2010) Acyl-CoA-binding protein 2 binds lysophospholipase 2 and lysoPC to promote tolerance to cadmium-induced oxidative stress in transgenic Arabidopsis. *Plant J.* **62**, 989–1003.

Geigenberger, P. (2003) Response of plant metabolism to too little oxygen. *Curr. Opin. Plant Biol.* **6**, 247–256.

Gibbs, D.J., Lee, S.C., Isa, N.M. *et al.* (2011) Homeostatic response to hypoxia is regulated by the N-end rule pathway in plants. *Nature*, **479**, 415–418.

Hinz, M., Wilson, I.W., Yang, J., Buerstenbinder, K., Llewellyn, D., Dennis, E.S., Sauter, M. and Dolferus, R. (2010) Arabidopsis *RAP2.2:* an ethylene response transcription factor that is important for hypoxia survival. *Plant Physiol.* **153**, 757–772.

Hsu, F.C., Chou, M.Y., Chou, S.J., Li, Y.R., Peng, H.P. and Shih, M.C. (2013) Submergence confers immunity mediated by the WRKY22 transcription factor in Arabidopsis. *Plant Cell*, **25**, 2699–2713.

Kieber, J.J., Rothenberg, M., Roman, G., Feldmann, K.A. and Ecker, J.R. (1993) *CTR1*, a negative regulator of the ethylene response pathway in Arabidopsis, encodes a member of the Raf family of protein kinases. *Cell*, **72**, 427–441.

Klok, E.J., Wilson, I.W., Wilson, D., Chapman, S.C., Ewing, R.M., Somerville, S.C., Peacock, W.J., Dolferus, R. and Dennis, E.S. (2002) Expression profile analysis of the low-oxygen response in Arabidopsis root cultures. *Plant Cell*, **14**, 2481–2494.

Leung, K.C., Li, H.Y., Xiao, S., Tse, M.H. and Chye, M.L. (2006) Arabidopsis ACBP3 is an extracellularly targeted acyl-CoA-binding protein. *Planta*, **223**, 871–881.

Li, H.Y. and Chye, M.L. (2004) Arabidopsis acyl-CoA-binding protein ACBP2 interacts with an ethylene-responsive element-binding protein, AtEBP, via its ankyrin repeats. *Plant Mol. Biol.* **54**, 233–243.

Li, H.Y., Xiao, S. and Chye, M.L. (2008) Ethylene- and pathogen-inducible Arabidopsis acyl-CoA-binding protein 4 interacts with an ethylene-responsive element binding protein. *J. Exp. Bot.* **59**, 3997–4006.

Li-Beisson, Y., Shorrosh, B., Beisson, F. *et al.* (2013) Acyl-lipid metabolism. *Arabidopsis Book*, **11**, e0161.

Licausi, F., van Dongen, J.T., Giuntoli, B., Novi, G., Santaniello, A., Geigenberger, P. and Perata, P. (2010) *HRE1* and *HRE2*, two hypoxia-inducible ethylene response factors, affect anaerobic responses in *Arabidopsis thaliana*. *Plant J.* **62**, 302–315.

Licausi, F., Kosmacz, M., Weits, D.A., Giuntoli, B., Giorgi, F.M., Voesenek, L.A.C.J., Perata, P. and van Dongen, J.T. (2011a) Oxygen sensing in plants is mediated by an N-end rule pathway for protein destabilization. *Nature*, **479**, 419–422.

Licausi, F., Weits, D.A., Pant, B.D., Scheible, W.R., Geigenberger, P. and van Dongen, J.T. (2011b) Hypoxia responsive gene expression is mediated by various subsets of transcription factors and miRNAs that are determined by the actual oxygen availability. *New Phytol.* **190**, 442–456.

Lynch, D.V. and Dunn, T.M. (2004) An introduction to plant sphingolipids and a review of recent advances in understanding their metabolism and function. *New Phytol.* **161**, 677–702.

Markham, J.E. and Jaworski, J.G. (2007) Rapid measurement of sphingolipids from *Arabidopsis thaliana* by reversed-phase high-performance liquid chromatography coupled to electrospray ionization tandem mass spectrometry. *Rapid Commun. Mass Spectrom.* **21**, 1304–1314.

Markham, J.E., Li, J., Cahoon, E.B. and Jaworski, J.G. (2006) Separation and identification of major plant sphingolipid classes from leaves. *J. Biol. Chem.* **281**, 22684–22694.

Markham, J.E., Molino, D., Gissot, L., Bellec, Y., Hématy, K., Marion, J., Belcram, K., Palauqui, J.C., Satiat-Jeunemaitre, B. and Faure, J.D. (2011) Sphingolipids containing very-long-chain fatty acids define a secretory pathway for specific polar plasma membrane protein targeting in Arabidopsis. *Plant Cell*, **23**, 2362–2378.

Mithran, M., Paparelli, E., Novi, G., Perata, P. and Loreti, E. (2013) Analysis of the role of the pyruvate decarboxylase gene family in *Arabidopsis thaliana* under low-oxygen conditions. *Plant Biol. (Stuttg)* **16**, 28–34.

Mortimer, J.C., Yu, X., Albrecht, S. *et al.* (2013) Abnormal glycosphingolipid mannosylation triggers salicylic acid-mediated responses in Arabidopsis. *Plant Cell*, **25**, 1881–1894.

Murashige, T. and Skoog, F. (1962) A revised medium for rapid growth and bio assays with tobacco tissue cultures. *Physiol. Plant.* **15**, 473–497.

Ohlrogge, J.B. and Browse, J. (1995) Lipid biosynthesis. *Plant Cell*, **7**, 957–970.

Perata, P. and Voesenek, L.A.C.J. (2007) Submergence tolerance in rice requires *Sub1A*, an ethylene-response-factor-like gene. *Trends Plant Sci.* **12**, 43–46.

Pucciariello, C., Parlanti, S., Banti, V., Novi, G. and Perata, P. (2012) Reactive oxygen species-driven transcription in Arabidopsis under oxygen deprivation. *Plant Physiol.* **159**, 184–196.

Raffaele, S., Vailleau, F., Léger, A., Joubès, J., Miersch, O., Huard, C., Blée, E., Mongrand, S., Domergue, F. and Roby, D. (2008) A MYB transcription factor regulates very-long-chain fatty acid biosynthesis for activation of the hypersensitive cell death response in Arabidopsis. *Plant Cell*, **20**, 752–767.

Ternes, P., Feussner, K., Werner, S., Lerche, J., Iven, T., Heilmann, I., Riezman, H. and Feussner, I. (2011) Disruption of the ceramide synthase LOH1 causes spontaneous cell death in *Arabidopsis thaliana*. *New Phytol.* **192**, 841–854.

Vailleau, F., Daniel, X., Tronchet, M., Montillet, J.L., Triantaphylidès, C. and Roby, D. (2002) A R2R3-MYB gene, *AtMYB30*, acts as a positive regulator of the hypersensitive cell death program in plants in response to pathogen attack. *Proc. Natl Acad. Sci. USA*, **99**, 10179–10184.

Voesenek, L.A.C.J. and Bailey-Serres, J. (2013) Flooding tolerance: O_2 sensing and survival strategies. *Curr. Opin. Plant Biol.* **16**, 647–653.

Wang, X. (2004) Lipid signaling. *Curr. Opin. Plant Biol.* **7**, 329–336.

Wang, W., Yang, X., Tangchaiburana, S. *et al.* (2008) An inositolphosphorylceramide synthase is involved in regulation of plant programmed cell death associated with defense in Arabidopsis. *Plant Cell*, **20**, 3163–3179.

Welti, R., Li, W., Li, M., Sang, Y., Biesiada, H., Zhou, H.E., Rajashekar, C.B., Williams, T.D. and Wang, X. (2002) Profiling membrane lipids in plant stress responses. Role of phospholipase Dα in freezing-induced lipid changes in Arabidopsis. *J. Biol. Chem.* **277**, 31994–32002.

Xia, Y., Yu, K., Gao, Q.M., Wilson, E.V., Navarre, D., Kachroo, P. and Kachroo, A. (2012) Acyl CoA binding proteins are required for cuticle formation and plant responses to microbes. *Front. Plant Sci.* **3**, 224.

Xiao, S. and Chye, M.L. (2009) An Arabidopsis family of six acyl-CoA-binding proteins has three cytosolic members. *Plant Physiol. Biochem.* **47**, 479–484.

Xiao, S. and Chye, M.L. (2011a) New roles for acyl-CoA-binding proteins (ACBPs) in plant development, stress responses and lipid metabolism. *Prog. Lipid Res.* **50**, 141–151.

Xiao, S. and Chye, M.L. (2011b) Overexpression of Arabidopsis ACBP3 enhances NPR1-dependent plant resistance to *Pseudomonas syringe* pv *tomato* DC3000. *Plant Physiol.* **156**, 2069–2081.

Xiao, S., Gao, W., Chen, Q.F., Chan, S.W., Zheng, S.X., Ma, J., Wang, M., Welti, R. and Chye, M.L. (2010) Overexpression of Arabidopsis acyl-CoA binding protein ACBP3 promotes starvation-induced and age-dependent leaf senescence. *Plant Cell*, **22**, 1463–1482.

Xue, Y., Xiao, S., Kim, J., Lung, S.C., Chen, L., Tanner, J.A., Suh, M.C. and Chye, M.L. (2014) Arabidopsis membrane-associated acyl-CoA-binding protein ACBP1 is involved in stem cuticle formation. *J. Exp. Bot.* **65**, 5473–5483.

Yang, C.Y. (2014) Hydrogen peroxide controls transcriptional responses of *ERF73/HRE1* and *ADH1* via modulation of ethylene signaling during hypoxic stress. *Planta*, **239**, 877–885.

Yang, C.Y., Hsu, F.C., Li, J.P., Wang, N.N. and Shih, M.C. (2011) The AP2/ERF transcription factor AtERF73/HRE1 modulates ethylene responses during hypoxia in Arabidopsis. *Plant Physiol.* **156**, 202–212.

Yurchenko, O.P. and Weselake, R.J. (2011) Involvement of low molecular mass soluble acyl-CoA-binding protein in seed oil biosynthesis. *New Biotechnol.* **28**, 97–109.

Zheng, S.X., Xiao, S. and Chye, M.L. (2012a) The gene encoding Arabidopsis acyl-CoA-binding protein 3 is pathogen inducible and subject to circadian regulation. *J. Exp. Bot.* **63**, 2985–3000.

Zheng, Y., Schumaker, K.S. and Guo, Y. (2012b) Sumoylation of transcription factor MYB30 by the small ubiquitin-like modifier E3 ligase SIZ1 mediates abscisic acid response in *Arabidopsis thaliana*. *Proc. Natl Acad. Sci. USA*, **109**, 12822–12827.